Supplementary Material (ESI) for Chemical Communications

Supplementary Materials

Metallothionein Fusion Proteins as a General Approach for Functionalized Protein Nanoparticle Assemblies

Marinella Sandros, De Gao, Cagil Gokdemir, and David E. Benson*
Department of Chemistry, Wayne State University, Detroit, MI 48202

N282C Maltose Binding Protein-Metallothionein (N282C MBP-MT) gene preparation: A DNA cassette encoding for the α-domain of *N. coriiceps* metallothionein was assembled and amplified by polymerase chain reaction on four oligonucleotides (Integrated DNA Technologies); 5'-GAA**GGATCC**AAGAGCTG-CTGCCCATGCTGCCCGTCGG-3', MT-sense-1; 5'-GCCGGAGGCGCATTTAGTACAACCCGACGGGCAGCA-3', MT-antisense-1; 5'-TGCGCCTCCGGCTGTGTGTGCAAAGGTAAAACCTGCGACACCT-CGT-3', MT-sense-2; 5'-CG**GGATCC**TTACTG-ACAGCACGAGGTGTCGCAGGT-3', MT-antisense-2. Each overlapping region (red, blue, and green underlines indicate complementary regions that nucleate oligonucleotide assembly) was designed to have a melting temperature of ~ 60 °C. A mixture of oligonucleotides (20 pmol, MT-sense-1 & MT-antisense-2; 0.2 pmol MT-antisense-1 & MT-sense-2) was amplified under standard conditions with *Taq* DNA polymerase through 30 cycles of 95 °C (1 min.), 55 °C (1. min), and 72 °C (2 min.). Restriction sites (*Bam HI*, bold letters in primers) on the resulting DNA fragment was digested with the *Bam HI* restriction enzyme (New England Biolabs), purified, and ligated into a maltose binding protein vector (New England Biolabs, pMal-C2) that had also been digested with *Bam HI*. The construct was then sequenced to confirm the production of a DNA sequence that codes for the metallothionein sequence on the carboxy-terminus of maltose binding protein through a Gly-Ser linker. The final product can be readily amplified and inserted between other restriction sites, as has been done with rat intestinal fatty acid binding protein (Gokdemir and Benson, unpublished results). DNA encoding for the surface N282C mutation in MBP-MT was prepared using two overlapping oligos (5'-TCCTCG-AAT**TGC**TATGCT-GA-3', sense; 5'-GTCAGCAGATA**GCA**TTCGAGGA-3', antisense; codon encoding the N282C mutation in bold) and amplification by 14 cycles of 95 °C (1 min.), 55 °C (1.

min), and 68 °C (14 min.) with *Pfu* DNA polymerase. The sequences of all constructs were confirmed by dideoxy sequencing using a Li-Cor sequencer.

Fluorophore attachment to N282C MBP-MT: N282C MBP-MT was purified to homogeneity by amylose chromatography (New England Biolabs) and dialyzed into in 20 mM MOPS Buffer at pH= 7.5. The necessity of tertiary amine buffers was found with Bodipy 577/618 maleimide, but not found when other fluorophores were used (*e.g.* PYMPO-maleimide, Molecular Probes). The protein sample was treated with 5 mM DTT , 10 mM EDTA, 1 mM 1,10-phenanthroline for 30 min. at 4°C and purified by gel-filtration chromatography (10-DG, Pharmacia). Addition of 100 μM $CdCl_2$ to the reduced and chelated sample was allowed to incubate at room temperature for 30 min., followed by the addition of 1.5 fold excess Bodipy 577/618 in DMF. After a two-hour incubation the reaction is quenched by the addition of ten fold molar excess of 2-mercaptoethanol and purified over a desalting column (10-DG, Pharmacia). Fluorophore modified N282C MBP-MT could be stored at 4 °C for at least two weeks at this stage. The fluorophore modified N282C MBP-MT was then treated with 0.1 mM EDTA and 0.1 mM 1,10-phenanthroline for 30 minutes. The chelated sample purified over a desalting column, concentration determined by absorbance at 280 nm, and used for soft nanoparticle labeling.

Proteolytic analysis of fluorophore introduction: Protein samples were dialyzed into a MOPS buffer (20 mM, pH 7.5). The fluorophore modified N282C MBP-MT was chelated and purified over a desalting column, as mentioned above. Before digestion the chelated sample was treated with 500 μM iodoacetic acid, reacted in the dark for 30 minutes, and then passed through a desalting column. Samples were thermally denatured at 90ºC for 10 min., cooled to room temperature, and digested with trypsin [Sigma, 50:1 (w/w)] at 37ºC for 4 hours or with chymotrypsin [Sigma, 60:1 (w/w)] at 25ºC for 6 hours. Typical concentrations at the digestion stage ranges from 5 to 20 μM, where 5 to 10 μL injections were made. HPLC separation was performed on a Waters 2695 module using a Waters Symmetry C_{18} column maintained at 25ºC. HPLC mobile-phase linear gradient (94:5:1 to 5:84:1 H_2O/MeCN/H_2O_2) was run over 30 minutes at a flow rate (0.4

mL/min.). Absorbance at 222 nm, 280 nm, and 575 nm were monitored, where the 575 nm absorbance directly reported any Bodipy 577/618 containing fragments. A single resolved peak in the 575 nm chromatograms were observed for the chymotrypsin and trypsin digested samples (Fig. S1).

Transmission electron microscopy of MBP-MT appended CdSe nanoparticles: MBP-MT attached THDA capped CdSe nanoparticle samples were analyzed by transmission electron microscopy (TEM). Drops of dilute samples (~ 10 nM) were placed on copper grids and allowed to evaporate overnight at room temperature. The TEM analysis was performed using a JEOL FastEM 2010 microscope operating at 200 kV. Size distribution was obtained by measuring the size of at least 100 particles on the TEM images. A histogram of nanoparticle sizes was then constructed to determine the nanoparticle size distribution. Example TEM images are shown in figure S2.

MBP-MT/CdSe Binding Kinetics: Equimolar mixtures of THDA capped CdSe and either MBP-MT or Bodipy 577/618 attached N282C MBP-MT, all at 800 nM, were incubated (room temperature, 24 hours) and analyzed by fluorescence emission intensities. Fluorescence intensities (363 nm excitation) and the ratio of Bodipy 577/618 to CdSe emission for the Bodipy 577/618 attached N282C MBP-MT samples were plotted as a function of time (Fig. S3). Increased CdSe emission intensity maximized in both samples at 4 hours, where the energy transfer ratio was approximately saturated after 24 hours for Bodipy 577/618 attached N282C MBP-MT CdSe THDA binding.

Bodipy 577/618 N282C MBP-MT affinity for THDA capped CdSe and CdSe/ZnS core-shell nanoparticles: Bodipy-577/618 modified N282C MBP-MT was titrated against 3.0-3.5 nm diameter CdSe and CdSe/ZnS core-shell nanoparticles. The ratio of the emission intensity at 620 nm (Bodipy 577/618) to emission intensity at 560 nm (CdSe or CdSe/ZnS), defined as I_{620}/I_{560}, was assumed to report binding progress. Changes in I_{620}/I_{560} as a function of protein concentration were fit to equation 1. Fig. S4 shows the changes in I_{620}/I_{560} as a function protein concentration and the fits to equation 1. The affinity for Bodipy-N282C MBP-MT binding to THDA capped CdSe was found to be

$6.3 \cdot 10^6$ M^{-1} (K_D = 160 nM) while the affinity for THDA capped CdSe/ZnS core-shell nanoparticles was found to be $1.3 \cdot 10^7$ M^{-1} (K_D = 80 nM).

Bodipy 577/618 N282C MBP-MT affinity for borate capped Au nanoparticles (Fig. S5): Bodipy-577/618 modified N282C MBP-MT was titrated against borate capped 2.0-4.0 nm Au nanoparticles. Literature methods[1] were used to prepare Au nanoparticles, via borohydride reduction of $HAuCl_4$. Size distribution of these nanoparticles was determined by TEM. Gravimetric analysis was used to prepare 50 nM solutions for titrations with Bodipy-577/618 modified N282C MBP-MT. The difference between Bodipy 577/618 fluorescence emission in samples with and without 50 nM Au nanoparticles was determined as a function of Bodipy-577/618 modified N282C MBP-MT concentration. A tight binding model was assumed; at high Au nanoparticle to Bodipy-N282C MBP-MT ratios all of the MBP-MT is bound to the nanoparticle. This assumption was evidenced by the large decrease in fluorescence intensity for the 0.1 nM Bodipy-N282C MBP-MT, 50 nM Au sample (Fig. S5A leftmost point). As the Bodipy-N282C MBP-MT concentration increases more free Bodipy-N282C MBP-MT is formed and diminishing the degree of Au mediated quenching. The mole fraction of Bodipy-577/618 modified N282C MBP-MT bound to Au nanoparticles (Au-MBP-MT) was determined by the difference of the maximal fluorescence difference initially observed and the fluorescence difference at twice the nanoparticle concentration. This mole fraction was multiplied by the concentration of Bodipy-577/618 modified N282C MBP-MT and plotted as function of [Au-MBP-MT] *vs* [Au-MBP-MT]/[MBP-MT]. Two slopes were observed and taken as $-1/K_A$, with the one associated with the higher MBP-MT reactions being a more accurate reflection of the binding affinity, which was determined as $3.1 \cdot 10^7$ M^{-1} (K_D = 32 nM, R = 0.975).

Concentration dependence of MBP-MT binding to THDA capped CdSe nanoparticles (Fig. S6): In order to address if a single or multiple non-interacting binding site[2] most accurately addressed MBP-MT binding to THDA capped CdSe nanoparticles, the concentration dependence of a derived association constants were studied. Reactions were performed at 1, 2 and 5 nM THDA capped CdSe, judged by previously derived

extinction coefficients.[3] If a single binding site model, as presumed by equation 1, best describes MBP-MT binding to THDA capped CdSe then association constants derived from MBP-MT titrations should be independent of THDA capped CdSe concentration. However, if the multiple non-interacting binding site model best fits MBP-MT binding to THDA capped CdSe nanoparticles, a linear increase in the derived association constants are expected. The association constant determined for MBP-MT binding to THDA capped CdSe nanoparticles was found to be $3.1 \cdot 10^9$ M^{-1} for 1 nM THDA capped CdSe nanoparticles, $1.2 \cdot 10^9$ M^{-1} for 2 nM THDA capped CdSe nanoparticles, and $2.2 \cdot 10^9$ M^{-1} for 5 nM THDA capped CdSe nanoparticles. Therefore a single binding site was found to model both MBP-MT binding to THDA capped CdSe nanoparticles. Such a finding is consistent with MBP being twice the size of the CdSe nanoparticles, thus any multiple binding site model would be expected to have interacting sites. Such an idea would be similar to the exchange kinetics and speciation of d^6 metal ions with aquo ligands. In this sense, the difference between our observations and previously reported[4, 5] MBP-His_5 binding interactions with CdSe and CdSe/ZnS core-shell nanoparticles may be due to the longer alkyl chain of the THDA capping groups providing substitutional inertness relative to the more solvent exposed lipoic acid capping groups.

Differences in FRET efficiencies with CdSe and CdSe/ZnS core/shell nanoparticles. The energy transfer observed in Bodipy-N282C MBP-MT with THDA capped CdSe nanoparticles was significantly higher than with THDA capped CdSe/ZnS core-shell nanoparticles. This difference (from ~ 9% efficiency to 5% efficiency) is a bit too large to be attributed to just the increase of Bodipy-CdSe distance (~ 3-4 Å). We propose that the additional perturbation in energy transfer efficiency comes from diminished contributions of CdSe surface states, relative to CdSe core states, to CdSe/ZnS emissive contributions to energy transfer. Additional studies are underway to demonstrate this hypothesis.

Different Bodipy-N282C MBP-MT and MBP-MT affinities for THDA capped CdSe nanoparticles. The association constant for Bodipy-N282C MBP-MT binding to THDA capped CdSe was four–fold weaker relative to MBP-MT. The decreased affinity has an decreased association rate for Bodipy-N282C MBP-MT. Prolonged incubation of

Bodipy-N282C MBP-MT with THDA capped CdSe nanoparticles, especially at high protein to nanoparticle ratios, resulted in precipitation after 72 hours. No precipitation was observed with unlabeled N282C MBP-MT or MBP-MT, suggesting that at least precipitation dependent on Bodipy addition to the system. This was further born out in the fact that robust labeling of Bodipy on N282C MBP-MT required the absence of phosphate due to blue precipitate formation and loss of protein. Such effects were not seen when the less hydrophobic PYMPO maleimide (Molecular Probes) was reacted with N282C MBP-MT. Therefore, we presume that the four-fold decrease in binding affinity with the addition of Bodipy to the MBP-MT-THDA capped CdSe nanoparticle system is due to Bodipy aggregation. Despite this aggregation, energy transfer was observed and aggregation could be minimized at moderate protein to nanoparticle ratios.

References:

1. G. T. Hermanson, *Bioconjugate Techniques,* Academic Press, San Diego, 1996, p.
2. A. Fersht, *Structure and Mechanism in Protein Science,* W. H. Freeman, New York, 1999, p. 207-209
3. W. W. Yu, L. H. Qu, W. Z. Guo and X. G. Peng. *Chemistry of Materials,* 2003, **15,** 2854-2860
4. A. R. Clapp, I. L. Medintz, J. M. Mauro, B. R. Fisher, M. G. Bawendi and H. Mattoussi. *Journal of the American Chemical Society,* 2004, **126,** 301-310
5. I. L. Medintz, A. R. Clapp, H. Mattoussi, E. R. Goldman, B. Fisher and J. M. Mauro. *Nature Materials,* 2003, **2,** 630-638

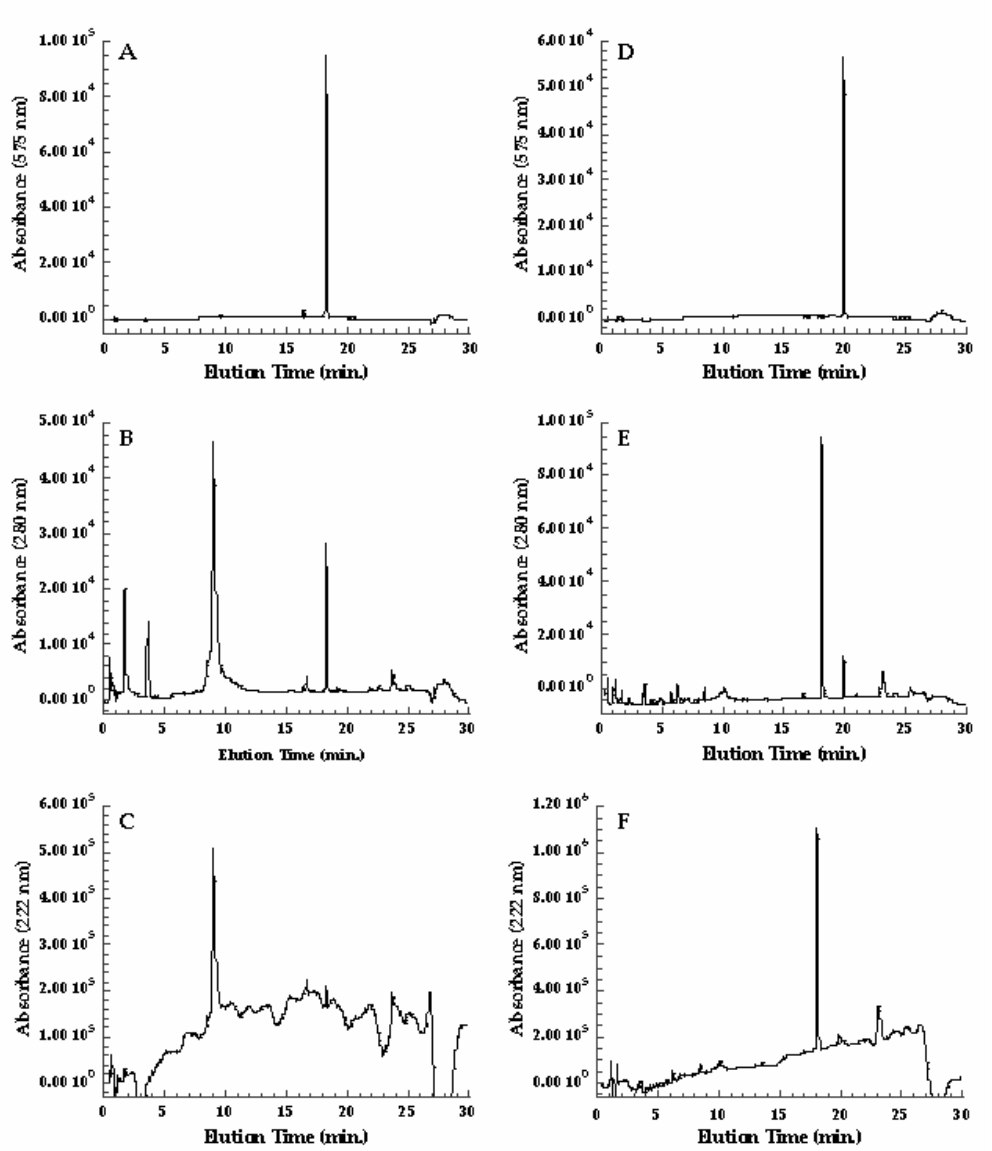

Fig S1. HPLC chromatograms of Trypsin (A-C) and Chymotrypsin (D-F) digested samples. Three wavelengths from these separations are shown: 575 nm (A, D); 280 nm (B, E); 222 nm (C, F).

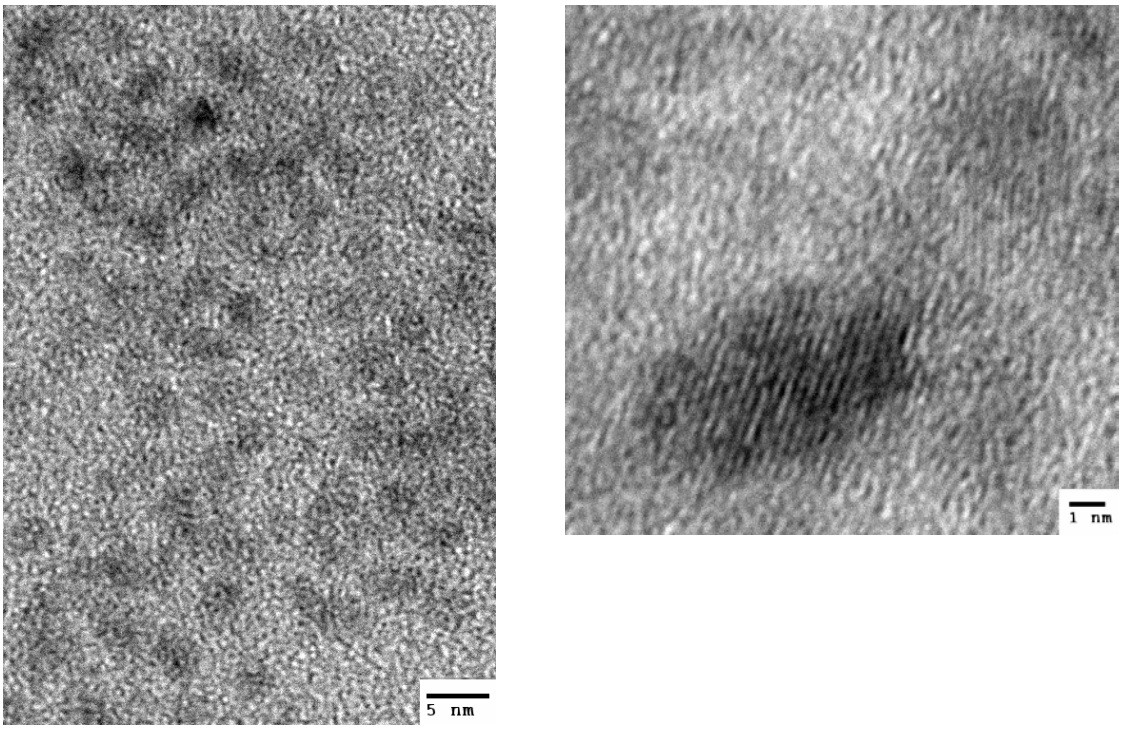

Figure S2. Example TEM micrographs of MBP-MT attached THDA capped CdSe nanoparticles at 250kX (left) and 800kX (above) magnification. The lattice spacing indicates the 202 face of cadmoselite CdSe.

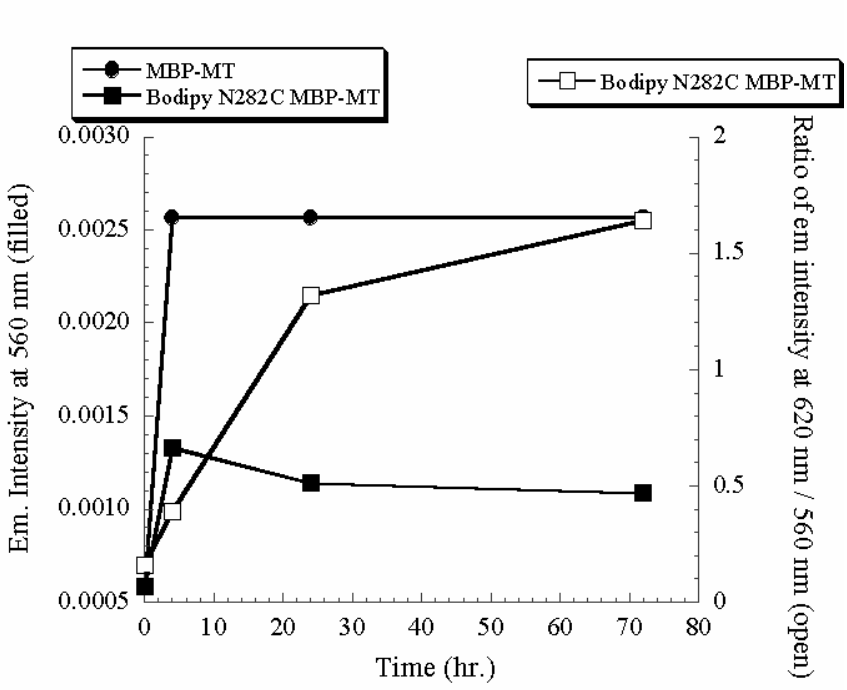

Figure S3. Kinetics of MBP-MT binding to THDA capped CdSe. Two samples were examined MBP-MT (filled circles) and Bodipy 577/618 labeled N282C MBP-MT (filled and open squares). Binding was observed either by increase in CdSe emission intensity (filled circles and squares, left axis) or by the ratio of Bodipy 577/618 to CdSe emission intensity (open squares, right axis).

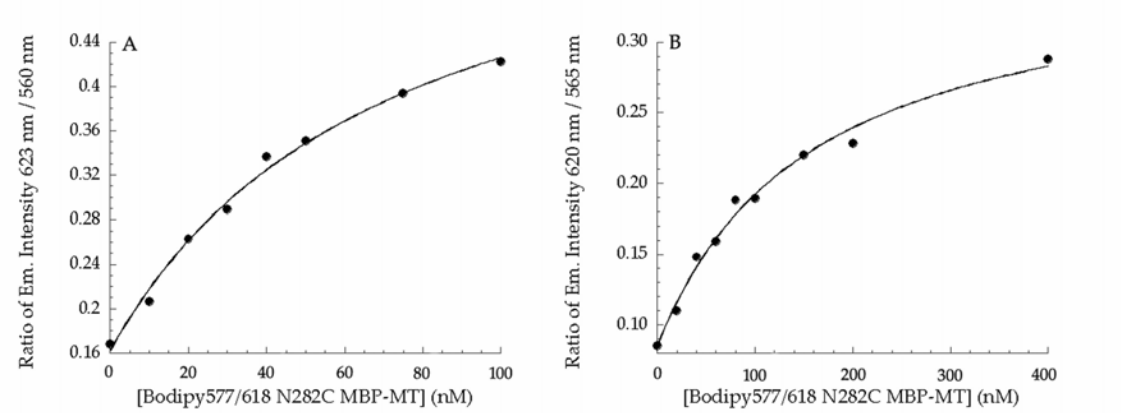

Figure S4. Changes in energy transfer as a function of Bodipy-N282C MBP-MT concentration. The data for the titration to THDA capped CdSe (A) and CdSe/ZnS core-shell (B) nanoparticles were fit to equation 1. The affinities derived from these data were $6.3 \cdot 10^6$ M^{-1} (K_D = 160 nM) for the CdSe titration and $1.3 \cdot 10^7$ M^{-1} (K_D = 80 nM) for the CdSe/ZnS titration.

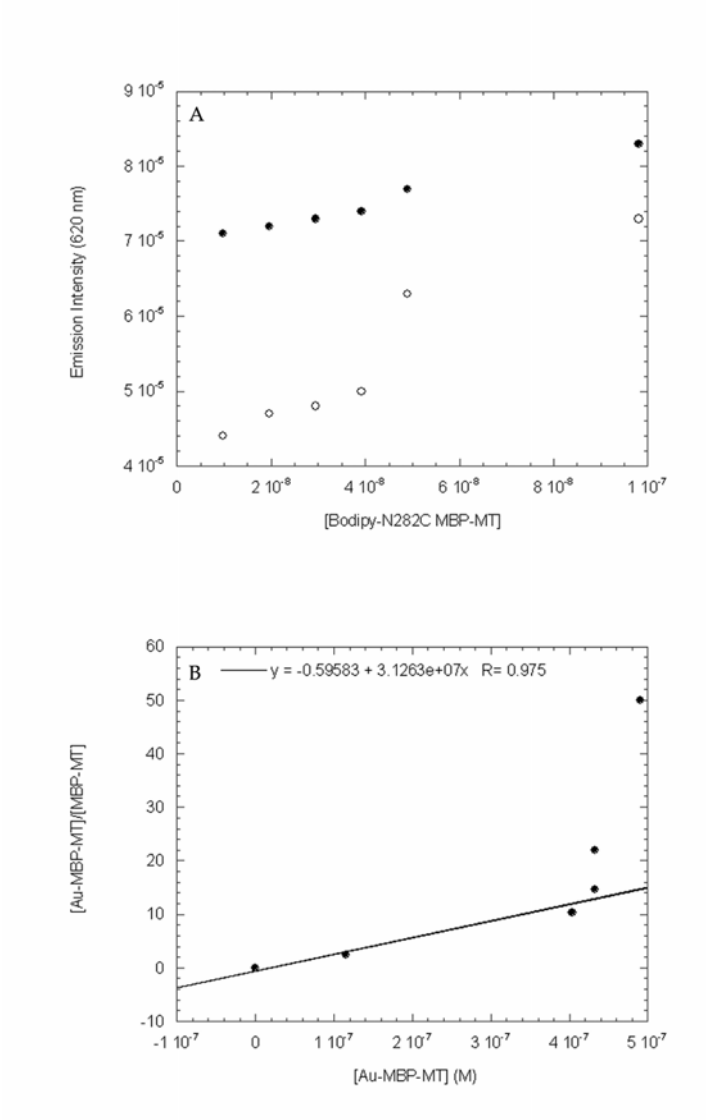

Fig. S5 Eadie-Hofstee analysis of MBP-MT affinity for borate capped 2.0-4.0 Au nanoparticles. A) Bodipy emission intensity as a function of Bodipy-N282C MBP-MT concentration; filled circles without Au nanoparticles, open circles with 50 nM Au nanoparticles. B) A tight binding model was assumed (see text) and used to determine the mole fraction of Au nanoparticle bound Bodipy-N282C MBP-MT from the degree of fluorescence quenching. The data in the plot of [Au-MBP-MT] *vs* [Au-MBP-MT]/[MBP-MT] was fit to two lines, and the slopes were taken as $1/K_A$, one beyond the tight binding limit ($5.4 \cdot 10^8$ M^{-1}; K_D = 2 nM) and another reflecting the MBP-MT affinity for Au nanoparticles ($3.1 \cdot 10^7$ M^{-1}; K_D = 32 nM).

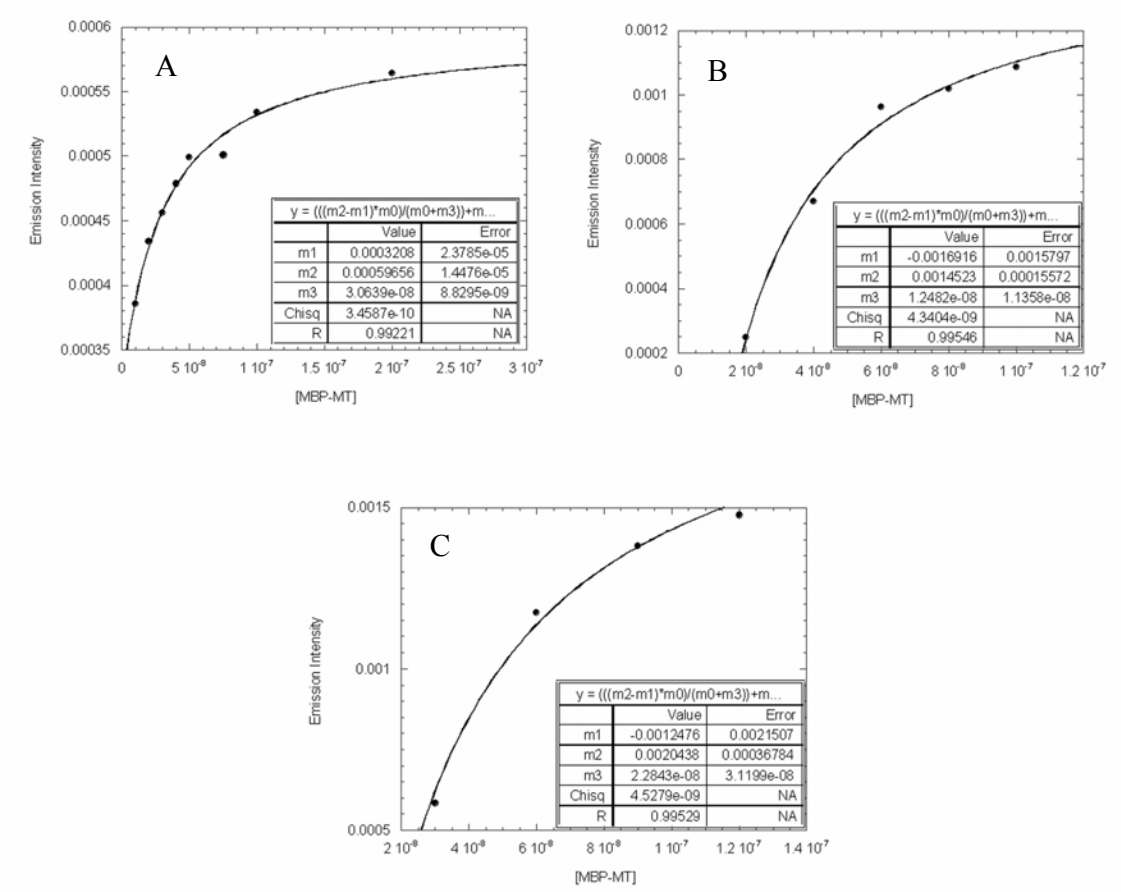

Figure S6. Concentration dependence of MBP-MT association constant determination. Three different THDA capped CdSe nanoparticle concentrations had MBP-MT titrations performed: A) 1 nM, B) 2 nM, and C) 5 nM. The association constant determined from the fits comes from 1/m3 and the average of these determinations (m3=$3.1\cdot10^{9}$, $1.2\cdot10^{9}$, and $2.2\cdot10^{9}$) yields an association constant of $4.7\pm0.7\cdot10^{7}$ M^{-1} (K_D = 21 nM).